

UCLA

UCLA Previously Published Works

Title

Core 1– and 3–derived O-glycans collectively maintain the colonic mucus barrier and protect against spontaneous colitis in mice

Permalink

<https://escholarship.org/uc/item/8nf5c960>

Journal

Mucosal Immunology, 10(1)

ISSN

1933-0219

Authors

Bergstrom, Kirk

Fu, Jianxin

Johansson, Malin EV

et al.

Publication Date

2017

DOI

10.1038/mi.2016.45

Peer reviewed

Core 1– and 3–derived O-glycans collectively maintain the colonic mucus barrier and protect against spontaneous colitis in mice

K Bergstrom¹, J Fu^{1,2}, MEV Johansson³, X Liu⁴, N Gao⁵, Q Wu^{1,6}, J Song¹, JM McDaniel¹, S McGee¹, W Chen⁵, J Braun⁷, GC Hansson³ and L Xia^{1,2,8}

Core 1– and 3–derived mucin-type O-glycans are primary components of the mucus layer in the colon. Reduced mucus thickness and impaired O-glycosylation are observed in human ulcerative colitis. However, how both types of O-glycans maintain mucus barrier function in the colon is unclear. We found that *C1galt1* expression, which synthesizes core 1 O-glycans, was detected throughout the colon, whereas *C3GnT*, which controls core 3 O-glycan formation, was most highly expressed in the proximal colon. Consistent with this, mice lacking intestinal core 1–derived O-glycans (IEC *C1galt1*^{−/−}) developed spontaneous colitis primarily in the distal colon, whereas mice lacking both intestinal core 1– and 3–derived O-glycans (DKO) developed spontaneous colitis in both the distal and proximal colon. DKO mice showed an early onset and more severe colitis than IEC *C1galt1*^{−/−} mice. Antibiotic treatment restored the mucus layer and attenuated colitis in DKO mice. Mucins from DKO mice were more susceptible to proteolysis than wild-type mucins. This study indicates that core 1– and 3–derived O-glycans collectively contribute to the mucus barrier by protecting it from bacterial protease degradation and suggests new therapeutic targets to promote mucus barrier function in colitis patients.

INTRODUCTION

Ulcerative colitis (UC) is a major form of inflammatory bowel disease characterized by chronic inflammation of the colon.¹ The etiology of UC remains unclear, but mounting evidence suggests it is initiated and promoted by abnormal interactions of epithelial and immune cells with the intestinal microbiota in genetically susceptible individuals.² Defective barrier function of colon mucus has emerged as a significant factor contributing to UC pathogenesis.³

The colon is colonized by a dense, complex microbiota primarily composed of bacteria ($\sim 10^{12}$ ml^{−1}).⁴ These microbiota are normally sequestered from the mucosa by a mucus layer overlying the intestinal epithelium.^{3,5} The structural basis of the mucus layer is a polymeric network primarily comprised

of the MUC2 mucin, which forms an inner stratified layer attached to the mucosal wall that is bacteria free, and a loosely attached outer layer that is colonized by the microbiota.^{6–8} MUC2 is extensively glycosylated with mucin-type O-linked oligosaccharides (O-glycans) that make up > 80% of its total mass.⁹ In UC patients, reduced mucus thickness and impaired O-glycosylation are reported.^{10,11} Muc2-deficient mice that lack a mucus layer develop spontaneous colitis,^{8,12} indicating an important role of Muc2 in mucus function and homeostasis.

O-glycans on Muc2 are of the core 1– and 3–derived type,¹³ which are built on the initial structure (GalNAc α -O-Ser/Thr, also called Tn antigen) within proline/serine/threonine-rich domains of the mucin protein core.¹⁴ The core 1 β 1,3-galactosyltransferase (C1GalT1), which is ubiquitously expressed, is

¹Cardiovascular Biology Research Program, Oklahoma Medical Research Foundation, Oklahoma City, Oklahoma, USA. ²Jiangsu Institute of Hematology, Collaborative Innovation Center of Hematology, Key Laboratory of Thrombosis and Hemostasis of Ministry of Health, The First Affiliated Hospital of Soochow University, Suzhou, China. ³Department of Medical Biochemistry, University of Gothenburg, Gothenburg, Sweden. ⁴The Second Affiliated Hospital, Central South University, Changsha, China. ⁵Department of Gastroenterology, The First Affiliated Hospital of Soochow University, Suzhou, China. ⁶Department of Biochemistry and Molecular Biology, School of Basic Medical Sciences, Fudan University, Shanghai, China. ⁷Department of Pathology and Laboratory Medicine, David Geffen School of Medicine, University of California, Los Angeles, California, USA and ⁸Department of Biochemistry and Molecular Biology, Oklahoma Center for Medical Glycobiology, University of Oklahoma Health Sciences Center, Oklahoma City, Oklahoma, USA. Correspondence: L Xia (Lijun-Xia@omrf.org)

Received 28 September 2015; accepted 30 March 2016; advance online publication 4 May 2016. doi:10.1038/mi.2016.45

solely responsible for the synthesis of core 1 *O*-glycans.¹⁵ In contrast, core 3 β 1,3-*N*-acetylglucosaminyltransferase (C3GnT), which controls the biosynthesis of core 3 *O*-glycans, is expressed mainly in the intestine and salivary glands.¹³ Both types of structures can be further extended and/or branched to form sialylated and/or sulfated core 1- or 3-derived *O*-glycans, such as core 2 or 4 *O*-glycans.^{16,17} Our previous studies show that mice lacking C3GnT (*C3GnT*^{-/-}) are more susceptible to chemically induced colitis,¹³ and intestinal epithelial cell-specific deletion of C1GalT1 (IEC *C1galt1*^{-/-}) leads to spontaneous colitis.¹¹ Yet, whether core 1 and 3 *O*-glycans differentially contribute to mucin barrier function and how *O*-glycans preserve mucus integrity remain unclear.

To address these questions, we generated a new mouse model that lacks both intestinal core 1- and 3-derived *O*-glycans (DKO). We found that core 3-derived *O*-glycans have an important role in the protective functions of mucus in the proximal colon where they are more highly expressed, and both types of *O*-glycans are required for colitis protection in the distal colon. Our results show that Muc2 requires both types of *O*-glycans to protect it from degradation by microbiota-derived proteolytic factors.

RESULTS

Core 1- and 3-derived *O*-glycans collectively contribute to mucus barrier function and colitis protection in the distal colon

To address whether core 1- and 3-derived *O*-glycans collectively contribute to mucus barrier integrity and colitis protection, we generated a new mouse line lacking intestinal core 1- and 3-derived *O*-glycans (DKO) by crossing IEC *C1galt1*^{-/-} mice with *C3GnT*^{+/-} mice (see **Supplementary Figure S1a** online). We compared colitis development of *C3GnT*^{-/-}, IEC *C1galt1*^{-/-}, and DKO mice with wild-type (WT) littermates.

Consistent with our published studies, *C3GnT*^{-/-} mice exhibited no colitis phenotype without challenge, and IEC *C1galt1*^{-/-} mice developed spontaneous colitis by 2 weeks of age.^{10,13} DKO mice started to develop spontaneous colon inflammation as early as postnatal day 8 (P8) (**Figure 1b** and see **Supplementary Figure S1b**), which progressed rapidly (**Figure 1a,b**). To determine whether a greater defect in the distal colonic mucus layer contributes to the earlier disease onset in DKO mice, we analyzed mucus layer structure in P7 WT and mutant mice, prior to colitis (**Figure 1b** and see **Supplementary Figure S1c**). Alcian blue (AB) staining of Carnoy's-fixed colonic sections revealed a clear inner stratified mucus layer in WT mice at P7, which was similar in *C3GnT*^{-/-} mice and even in IEC *C1galt1*^{-/-} mice at this age; in contrast, the inner mucus layer thickness was significantly reduced in DKO mice (**Figure 1c,d**). Immunohistochemistry (IHC) for Tn antigen, exposed when lacking both core 1 and 3 *O*-glycans, confirmed the presence of truncated *O*-glycans in goblet cells and the inner mucus layer of IEC *C1galt1*^{-/-} and DKO littermates (**Figure 1e,f**).

To investigate whether the impaired mucus layer impacted tissue-microbiota interactions, we performed dual staining for the major colonic mucin Muc2 and luminal bacteria via fluorescence *in situ* hybridization (FISH) with the universal bacterial probe EUB338. A progressive reduction of the mucus barrier between the microbiota and the mucosal surface was observed in DKO mice vs. all other groups (see **Supplementary Figure S1d**). At P12, bacteria were in direct contact with the mucosa in the DKO colon (**Figure 1g**). An intestinal permeability assay using fluorescein isothiocyanate-dextran (FD4, 4kDa) revealed a significant increase in barrier permeability in both IEC *C1galt1*^{-/-} and DKO mice relative to WT mice (**Figure 1h**). By P21, the mucus layer was absent in DKO mice and dramatically reduced in IEC *C1galt1*^{-/-} mice compared with WT and *C3GnT*^{-/-} mice (**Figure 1d**). At this time point, colitis was most severe in DKO mice, evidenced by histological scoring, elevated proinflammatory cytokine expression, and polymorphonuclear cell infiltration (**Figure 1b**, see **Supplementary Figure S1e,f**). Collectively, these results indicate that the degree of intestinal *O*-glycan loss is directly correlated with the level of mucus layer impairment as well as colitis onset and severity.

Loss of both core 1- and 3-derived *O*-glycans affects mucus layer structure and colitis susceptibility throughout the colon

Although core 1 *O*-glycosylation is most important for mucus barrier function in the distal colon, whether this is the case in the proximal colon was unclear. To address this, we compared disease and *O*-glycosylation status in the proximal colon of WT and IEC *C1galt1*^{-/-} mice. Relative to the distal colon, *O*-glycosylation was intact in goblet cells, a mucus layer was visible, and colitis was minimal in the proximal colon of 3-month-old IEC *C1galt1*^{-/-} mice vs. WT littermates based on AB staining (see **Supplementary Figure S2a-d**). We therefore hypothesized that core 3-derived *O*-glycans protect IEC *C1galt1*^{-/-} proximal colon from spontaneous disease. Gene expression analysis of enriched colon crypt cells by quantitative reverse transcriptase-PCR (RT-qPCR) showed higher levels of *C3GnT* expression in the proximal colon of WT and IEC *C1galt1*^{-/-} mice than that of the distal colon (**Figure 2a**), consistent with AB staining (see **Supplementary Figure S2**); in contrast, *C1galt1* was expressed at similar levels in the proximal and distal colon of WT mice but not of IEC *C1galt1*^{-/-} mice as expected (**Figure 2a**). These results show a differential expression pattern of *C3GnT* in different regions of the murine colon.

To show that both core 1- and 3-derived *O*-glycans contribute to mucus layer integrity in the proximal colon, we compared glycosylation, mucus layer, and disease status of this region between 3-month-old WT, *C3GnT*^{-/-}, IEC *C1galt1*^{-/-}, and DKO mice. IHC for Tn antigen revealed that the percentage of Tn-positive (Tn⁺) proximal goblet cells was 100% in DKO mice, compared with ~50% Tn⁺ in IEC *C1galt1*^{-/-} mice, and no Tn⁺ goblet cells in WT and *C3GnT*^{-/-} mice (**Figure 2b**). In contrast, distal colonic Tn expression was comparable between IEC *C1galt1*^{-/-} and DKO mice at this age (see

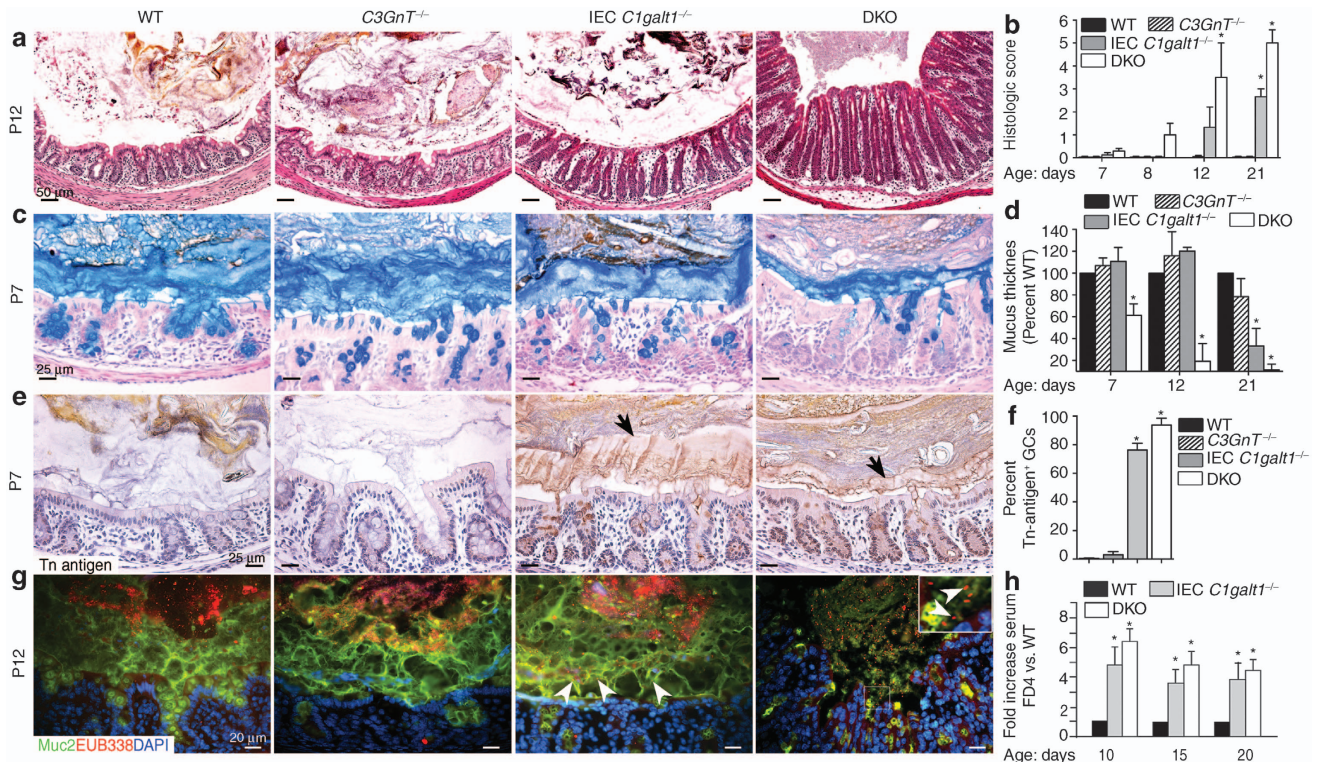


Figure 1 DKO mice have early onset and more severe colitis in the distal colon. (a) Representative images of hematoxylin and eosin-stained distal colons. P12 = postnatal day 12. (b) Histological colitis score. (c) Representative Alcian blue staining of Carnoy's-fixed colonic sections. (d) Quantification of mucus thickness vs. wild-type (WT) mice. Error bars = s.e.m. (e) Representative images of Tn antigen immunohistochemistry (brown) in colon sections. Arrow: top of mucus layer. (f) Quantification of Tn⁺ cells from mice in (e). (g) Representative dual staining for Muc2 (immunofluorescence, green) and bacteria (fluorescence *in situ* hybridization, red), the latter using the universal EUB338 probe, on Carnoy's-fixed colonic sections. Inset, magnified image of boxed region. Arrowheads, bacteria. (h) Quantitation of serum fluorescein isothiocyanate-Dextran, 4 kDa 4 h after oral administration. Bars show average fold changes relative to WT mice. Data are representative of >2 independent studies with $n = 4-6$ mice per group. For **b**, **d**, and **h**, * $P < 0.05$ vs. WT.

Supplementary Figure S3). To examine the relationship between Tn expression patterns and proximal colon mucus layer integrity, we immunostained Carnoy's-fixed colon tissues (with stool intact) of each strain for Muc2 and compared inner mucus layer structure. WT and C3GnT^{-/-} mice showed a Muc2-rich inner mucus layer separating luminal content from the mucosa; IEC C1galt1^{-/-} mice had reduced thickness of the inner mucus layer and DKO mice had a complete loss of the layer (Figure 2c,d). To determine whether this impacted colitis susceptibility, we analyzed hematoxylin and eosin-stained colon sections. Spontaneous inflammation in proximal colon regions was observed in DKO but not in WT, C3GnT^{-/-}, and IEC C1galt1^{-/-} mice (Figure 2e,f). Thus, whereas colitis protection in the distal colon is primarily dependent on core 1 O-glycans, both core 1- and 3-derived O-glycans cooperate in the proximal colon to preserve mucus barrier integrity.

Both core 1- and 3-derived O-glycans contribute to mucus layer establishment and colitis protection in adult mice

Our data show that constitutive loss of O-glycans during embryonic and postnatal development affects mucus layer structure and colitis severity, but it was not clear whether loss of intestinal O-glycans during adulthood would have

similar consequences. To address this question, previously described mice with tamoxifen (TM)-inducible deficiency of C1GalT1 (TM-IEC C1galt1^{-/-})¹⁰ on a C3GnT^{+/+} background were bred with C3GnT^{+/+} mice to generate WT, TM-IEC C1galt1^{-/-}, and TM-DKO littermates (Figure 3a). We treated 10–12-week-old littermate WT, TM-IEC C1galt1^{-/-}, and TM-DKO with TM for 5 consecutive days and killed all mice 5 and 10 days after final TM treatment for mucus and disease analysis (Figure 3b). By histology, colitis occurred in both TM-IEC C1galt1^{-/-} and TM-DKO mice, although it was most severe in TM-DKO mice at 5 and especially 10 days post-TM (Figure 3c,d). To determine the relationship of colitis onset to the mucus layer, we performed AB staining. A loss of AB-stained mucus layer was obvious in the distal colon of TM-DKO mice by 5 days, compared with WT and TM-IEC C1galt1^{-/-} littermates, the latter still showing a thin mucus layer even at 10 days post-TM (Figure 3d,e). Immunofluorescent (IF) staining for Muc2 and Tn antigen revealed that most goblet cells in the distal colon of both strains expressed mucin with truncated O-glycans (i.e., dually Muc2⁺Tn⁺) (Figure 3e,f). However, some TM-IEC C1galt1^{-/-} mice at 5 days post-TM, and to a lesser extent at 10 days post-TM, showed a mixed Tn⁺ and Tn-negative (Tn⁻) inner mucus layer, with the truncated O-glycan

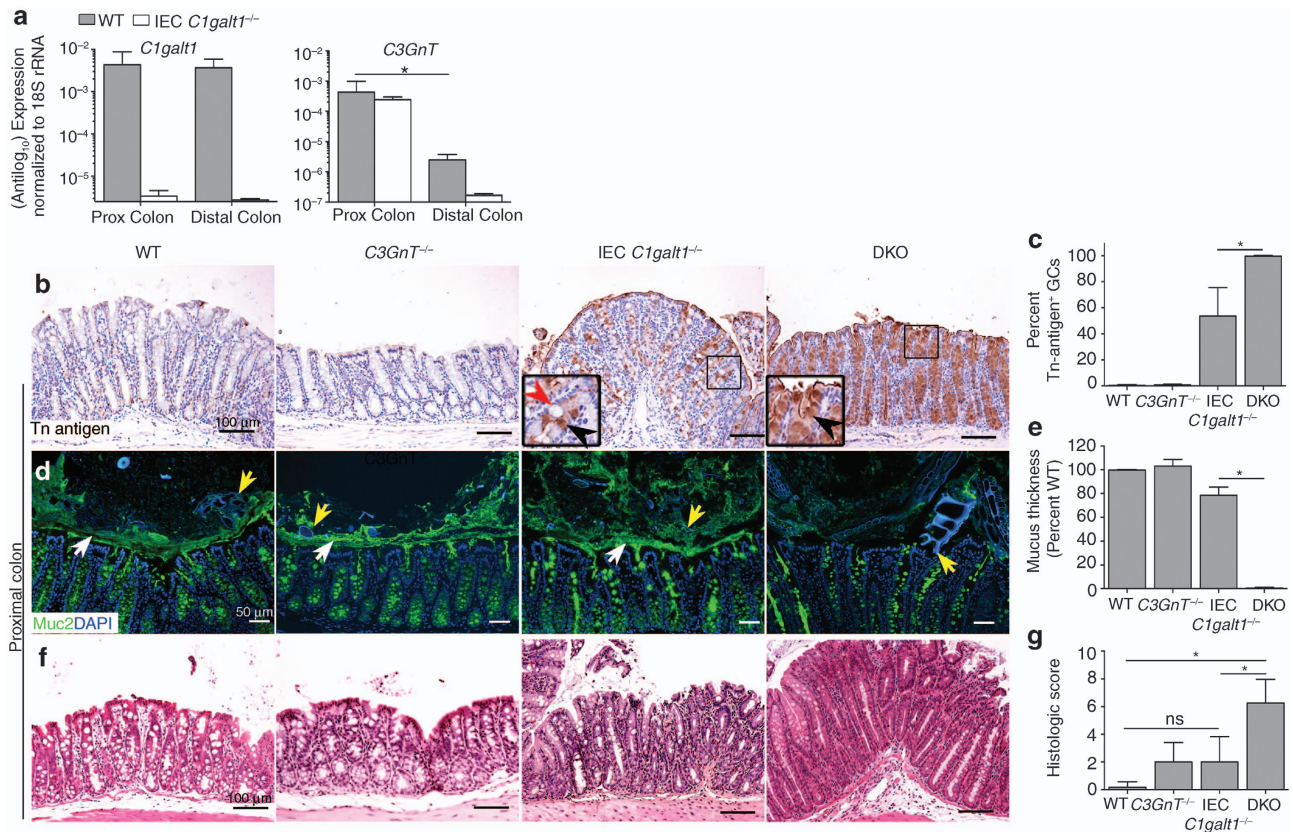


Figure 2 DKO mice exhibit defective mucus and spontaneous colitis in the proximal colon. **(a)** Gene expression analysis of enriched colonic crypt cells by quantitative reverse transcriptase–PCR. **(b)** Representative immunohistochemistry for Tn antigen (brown). Inset, magnified image of boxed regions. Arrowheads: red, Tn⁻ goblet cell; black, Tn⁺ goblet cell. **(c)** Quantification Tn⁺ goblet cells. Error bars = s.e.m. **(d)** Representative immunofluorescent staining for Muc2 on Carnoy's-fixed sections. Arrows: White, mucus layer; yellow, luminal food particle. **(e)** Quantification of mucus thickness vs. wild-type (WT) mice. **(f)** Representative hematoxylin and eosin staining of proximal colonic sections. **(g)** Histological colitis score. Data are representative of two independent studies, $n = 4$ – 6 per group; WT mice are littermate controls. * $P < 0.05$, Student's t -test for **a**, **c**, and **e**, and one-way analysis of variance with Bonferroni post-test for **g**.

(i.e., Tn⁺) portion being contributed directly by mucosal goblet cells (**Figure 3e**), suggesting core 3 O-glycans on the luminal side were somehow protecting its loss. In the proximal colon, AB staining intensity was lower in TM-DKO vs. TM-IEC *C1galt1*^{-/-} mice (see **Supplementary Figure S4a**). Dual Muc2/Tn staining revealed that a greater fraction of proximal colonic goblet cells were expressing truncated O-glycans on mucin (i.e., Muc2⁺Tn⁺) in TM-DKO mice vs. TM-IEC *C1galt1*^{-/-} mice, while all proximal goblet cells in WT mice harbored normal mucin (i.e., Tn⁻) in their secretory granules (see **Supplementary Figure S4c,d**). Consistent with this, the proximal colon mucus layer of TM-IEC *C1galt1*^{-/-} mice showed mixed Tn expression, whereas this layer vanished in TM-DKO mice (see **Supplementary Figure S4b,c**). These results indicate that core 3-derived O-glycans contribute to mucus layer integrity and affect colitis development after induced deletion of core 1 O-glycans in adult mice.

Antibiotic treatment rescues the mucus layer and reduces severity of colitis in DKO mice

To address whether an inner mucus defect leads to increased bacterial interactions with the epithelium and subsequently

contributes to colitis, WT and DKO mice were treated with broad-spectrum antibiotics (neomycin sulfate, metronidazole, vancomycin, ampicillin (NMVA)) for 4 weeks (**Figure 4a**),^{10,18} followed by mucus layer structure and disease analysis. As expected, NMVA significantly reduced bacterial levels in NMVA- vs. vehicle-treated mice, as tested by qPCR of bacterial 16S rRNA for total bacteria, and for bacterial subsets belonging to different phyla (**Figure 4b**). Dual Muc2 IF/EUB338 FISH analysis revealed that, in the vehicle-treated groups, bacteria were in direct contact with the mucosa in DKO mice, which lacked a mucus layer, whereas bacteria were separated from epithelia by an inner mucus layer in WT mice (**Figure 4c**). In the NMVA-treated groups, EUB338 signal was not detected, and a thick inner layer mucus was maintained in WT mice; in addition, a thin mucus layer was also observed in DKO mice (**Figure 4c**). To determine whether the improved mucus layer in treated DKO mice resulted from the presence of intact mucins, we extracted colon luminal mucus scrapes and analyzed them via composite agarose-polyacrylamide gel electrophoresis (AgPAGE)¹⁹ followed by in-gel periodic acid/Schiff (PAS staining), which stains neutral as well as acidic mucins. Vehicle-treated WT mice had a strong 1–2-MDa

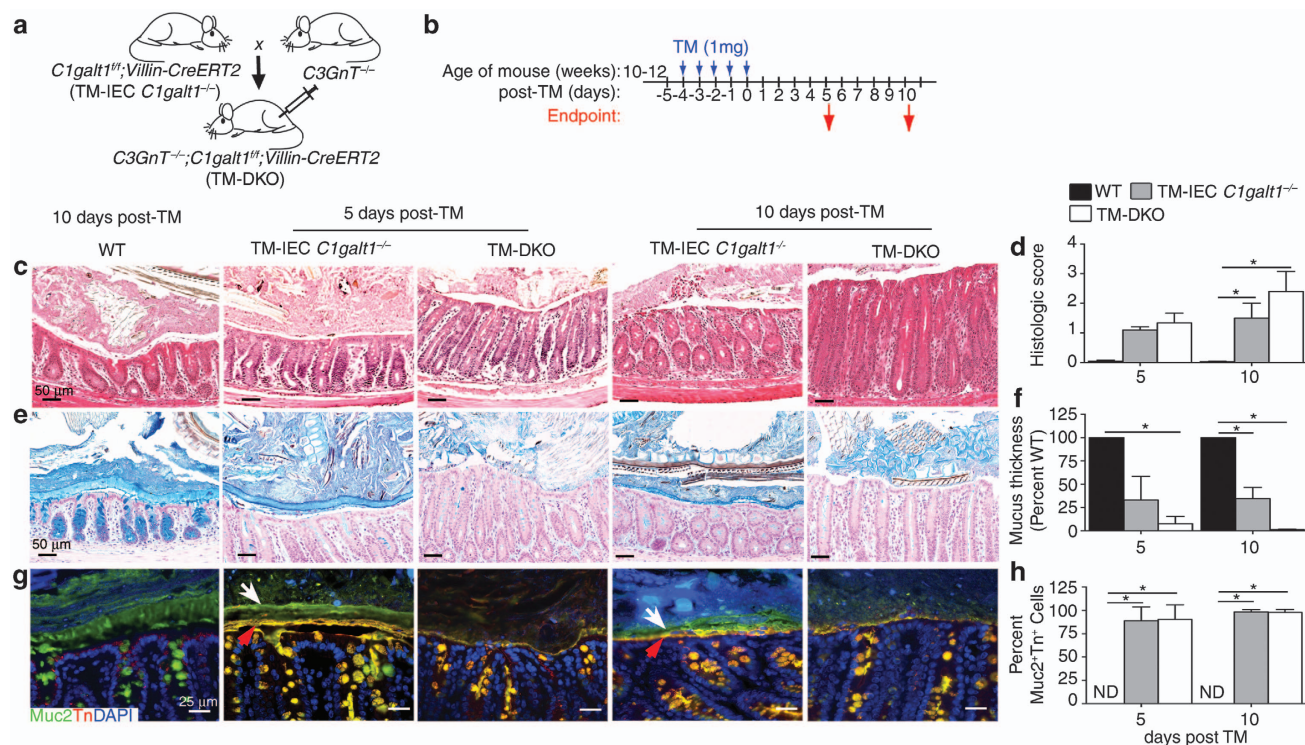


Figure 3 Deficiency of core 1- and 3-derived O-glycans impairs mucus layer and causes colitis in adult mice. (a) Generation of inducible DKO mice. (b) Experimental design. (c) Hematoxylin and eosin staining of Carnoy's-fixed distal colon sections. (d) Histological colitis score. (e) Representative Alcian blue staining on Carnoy's-fixed colon sections. (f) Quantification of mucus thickness vs. wild-type (WT) mice (from Muc2 stain). (g) Dual immunofluorescence for Muc2 (green) and Tn antigen (red); dual Muc2⁺ Tn⁺ cells are yellow (white arrow). Arrowheads: white, Tn⁻ portion of mucus; red, Tn⁺ portion of mucus. (h) Quantification of dual Muc2⁺ Tn⁺ cells. For all bar graphs, error bars = s.e.m. Results are representative of two independent experiments, $n = 4-6$ mice per group per time point. Tamoxifen (TM)-treated WT littermates are experimental controls. * $P < 0.05$ vs. TM-treated WT mice, one-way analysis of variance with Bonferroni post-test.

band but only a faint band was detected in vehicle-treated DKO mice. In contrast, a high molecular weight (MW) band was evident in NMVA-treated DKO secretions, migrating between the two major bands in WT mice (Figure 4d).

We next investigated how loss of O-glycans impaired mucin stability. Although mucus Muc2 is primarily modified by O-glycans, N-glycans are present in the C-terminal cysteine knot of human and rodent Muc2. Fucose (Fuc) is a common capping structure on both O- and N-glycans. In DKO mice, O-glycans are truncated to Tn antigen and thus do not carry any Fuc; however, Fuc on N-glycans of Muc2 should not be affected.²⁰ Therefore, Fuc can be used as a marker for monitoring the stability of Muc2. We used the lectin *Ulex europaeus* agglutinin-1 (UEA1, binds Fuc α 1,2Gal epitopes) to stain the tissue and found that luminal UEA1 was detected in WT mucus as expected (Figure 4e). NMVA-treated WT showed a slightly increased UEA1 staining, suggesting that some Fuc on O- or N-glycans are susceptible to bacteria-mediated degradation. In contrast, no luminal UEA1 was seen in the DKO tissue; however, similar to Muc2 staining, a thin UEA1-rich layer was observed overlying the mucosal surface of NMVA-treated DKO mice (Figure 4e). These results support that bacteria-derived enzymes digest O-glycan-deficient mucins even in the presence of N-glycans as monitored by Fuc labeling. Notably, colitis severity was dramatically reduced in NMVA-treated

DKO mice (Figure 4f). Collectively, these studies indicate that O-glycans are critical for mucin stability and a partial rescue of the mucus layer in DKO mice is associated with amelioration of inflammation and suggest that colitis is driven by bacterial-mucosal interactions following mucus barrier breach.

Loss of the mucus barrier in DKO mice is dependent upon the microbiota but not inflammation

Both inflammation and microbiota may affect mucus structure and glycosylation.^{11,19} To determine whether loss of the mucus layer in DKO mice is caused by bacterial factors prior to inflammation, we orally administered a high dose (20 mg) of the aminoglycoside antibiotic streptomycin (strep) to WT and DKO mice once a day for 2 days and then analyzed these mice for mucus integrity (Figure 5a). This antibiotic was chosen owing to its rapid action^{21,22} and broad-spectrum activity at high doses against many Gram-negative and -positive facultative anaerobes²³ as well as obligate anaerobes such as *Bacteroides*.²⁴ Indeed, qPCR analysis of fecal content revealed that this treatment led to an approximately a 1000-fold drop in total microbiota (Figure 5b), and a 10,000 fold decrease in the Bacteroidales order, in DKO mice (Figure 5c). The overall reduction in total microbiota was confirmed independently by FISH analysis of colonic cross-sections (Figure 5d). Importantly, the severity of colitis between strep-treated

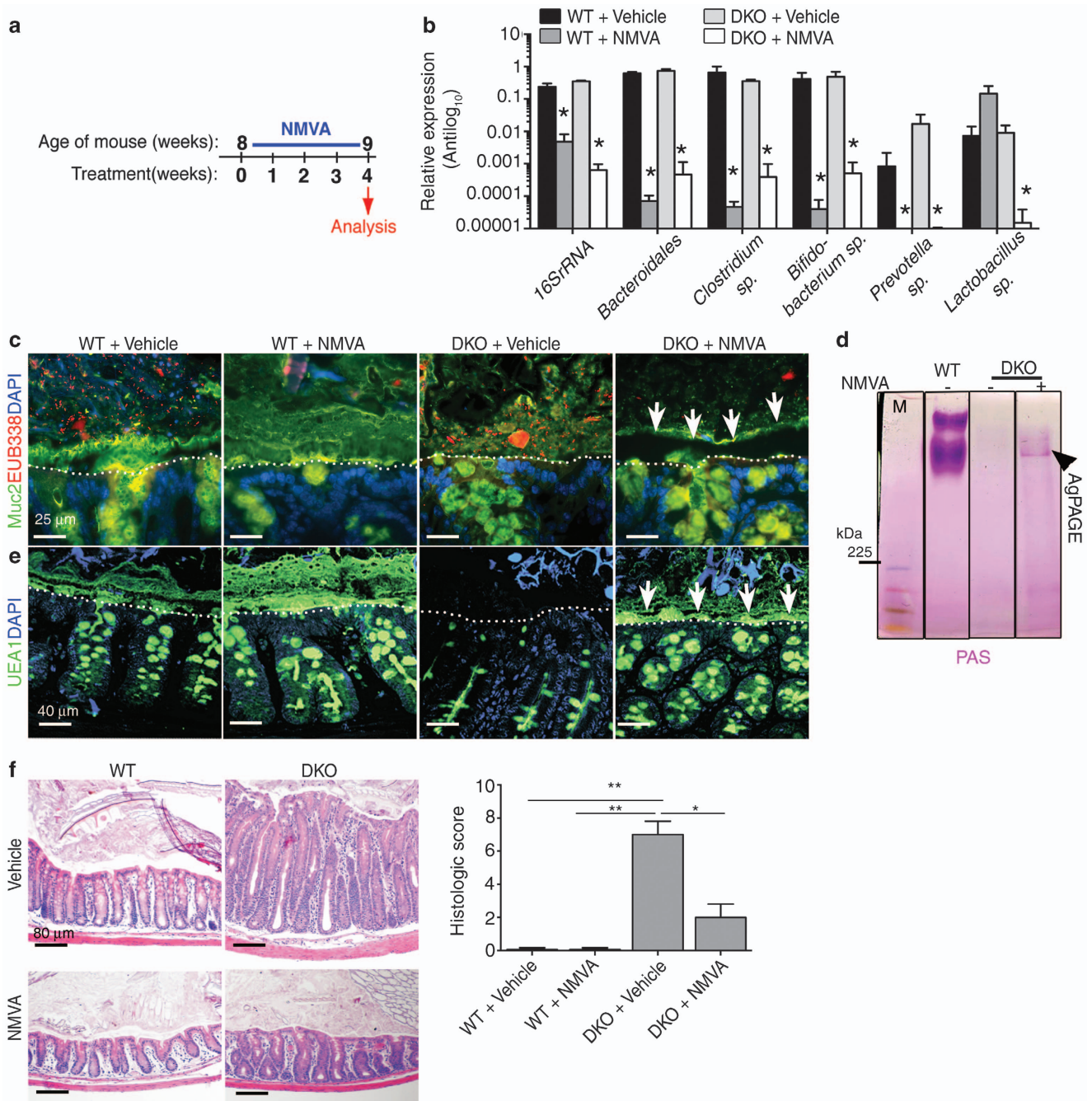


Figure 4 Microbial depletion rescues defective mucus layer function and ameliorates colitis in DKO mice. **(a)** Experimental design. **(b)** Quantitative PCR of bacterial universal and group-specific 16S RNA gene from fecal gDNA. **(c)** Representative dual Muc2/EUB33 staining. Arrow, mucus layer. **(d)** Composite agarose-polyacrylamide gel electrophoresis analysis of semipurified murine colonic mucin, visualized by periodic acid/Schiff staining (magenta). Arrow, mucin band in DKO. **(e)** Immunofluorescent staining for the lectin *Ulex europaeus* agglutinin-1. Arrow, mucus layer. **(f)** Representative hematoxylin and eosin staining of distal colon sections. Right: histological damage score. Results are representative of two independent experiments, $n = 4$ mice per group. Wild-type (WT) mice are experimental controls. * $P < 0.05$ and ** $P < 0.01$ vs. vehicle-treated WT, one-way analysis of variance with Bonferroni post-test.

and non-treated mice was no different owing to the short time frame of antibiotic treatment (**Figure 5e**). However, strep-treated DKO mice exhibited a clear and obvious Tn⁺ mucus layer, whereas no visible mucus layer was found overlying the surface on untreated DKO mucosa (**Figure 5f**). To investigate whether strep treatment rescues Muc2/mucus quantitatively,

we extracted mucus secretions of untreated or strep-treated WT and DKO mice, separated them via AgPAGE, and visualized them by PAS staining. Consistent with the Muc2 staining on colonic cross-sections, we found a more intensely PAS-stained high MW band in strep-treated DKO mice vs. untreated mice (**Figure 5g**).

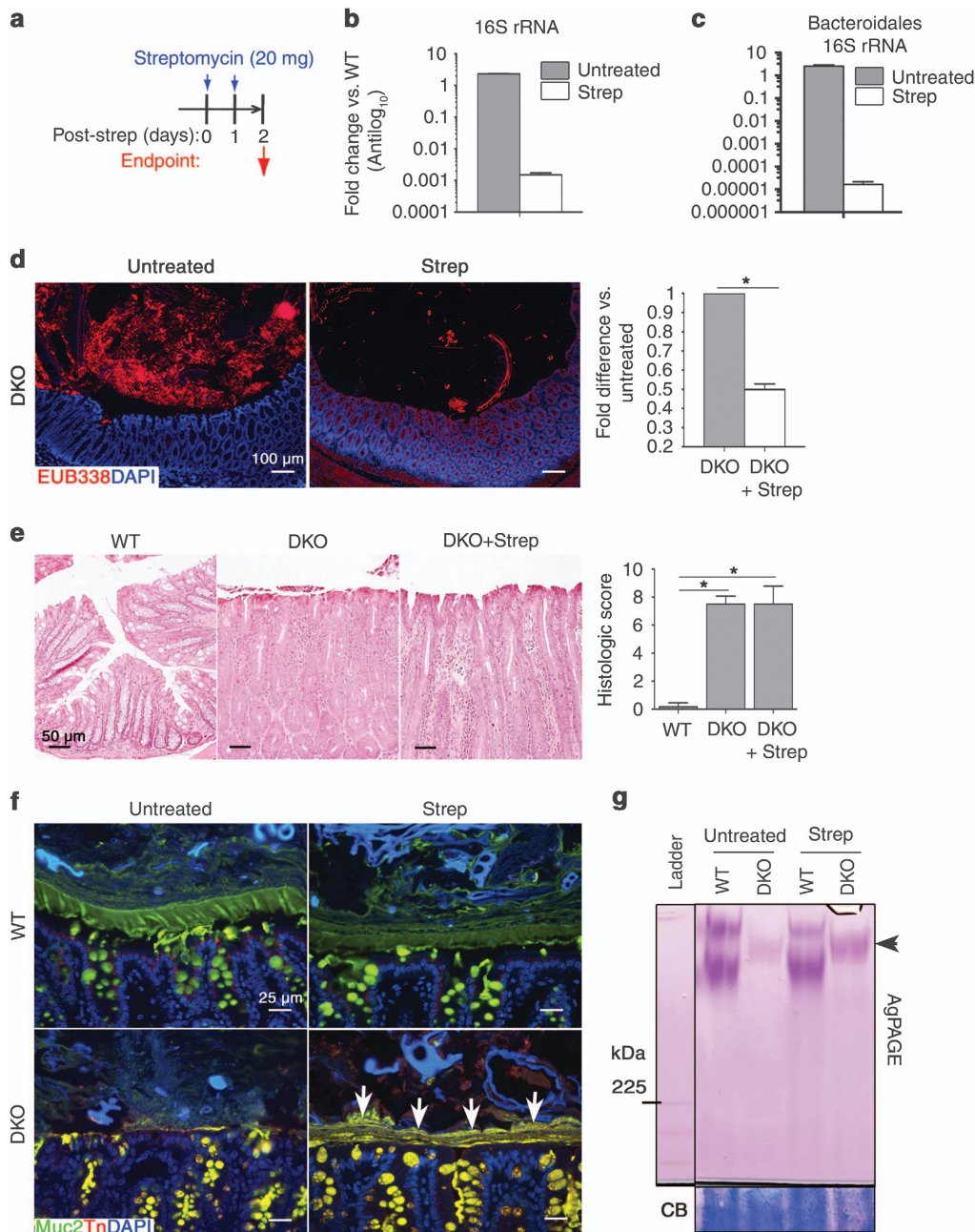


Figure 5 Loss of the mucus barrier in DKO-deficient mice is dependent upon the microbiota but not inflammation. (a) Experimental design for short-term microbial depletion. (b) Quantitative PCR (qPCR) of total bacterial universal 16S rRNA gene. (c) qPCR of bacterial 16S rRNA gene specific for Bacteroidales order. (d) Representative fluorescence *in situ* hybridization (FISH) using EUB338 to stain bacteria (red). Right: Relative quantification of FISH signal in lumen. (e) Representative hematoxylin and eosin of distal colon tissues. Right: histological damage score. (f) Dual immunofluorescence for Muc2 (green) and Tn antigen (red) on Carnoy's-fixed colonic sections. Arrows, dual Muc2⁺Tn⁺ mucus layer. (g) Composite agarose-polyacrylamide gel electrophoresis analysis of semipurified murine colonic mucin, visualized by periodic acid/Schiff staining (magenta). Arrow, DKO Muc2 mucin band. CB, Coomassie Blue loading control. Results are representative of three independent experiments, 3–6 mice per group. Non-treated wild type or DKO are experimental controls. * $P < 0.05$, Student's *t*-test.

O-glycans protect Muc2 from bacterial protease-mediated degradation

The above results suggest that the loss of mucus layer integrity in O-glycan-deficient mice is largely dependent on the microbiota but independent of inflammation. Indeed, bacteria could be seen between a broken, discontinuous mucus layer remaining in some DKO mice, in contrast to a continuous

mucus layer in NMVA-treated DKO mice (Figure 6a). Although bacterial glycosidases, sulfatases, and proteases may contribute to mucus layer breakdown,^{19,25,26} we hypothesized that proteases have a major role. We tested this directly by treating mucus extracted from strep-treated WT and DKO mice with or without pronase, a mixture of proteases derived from *Streptococcus* sp., (1 mU for 30 min). Subsequent

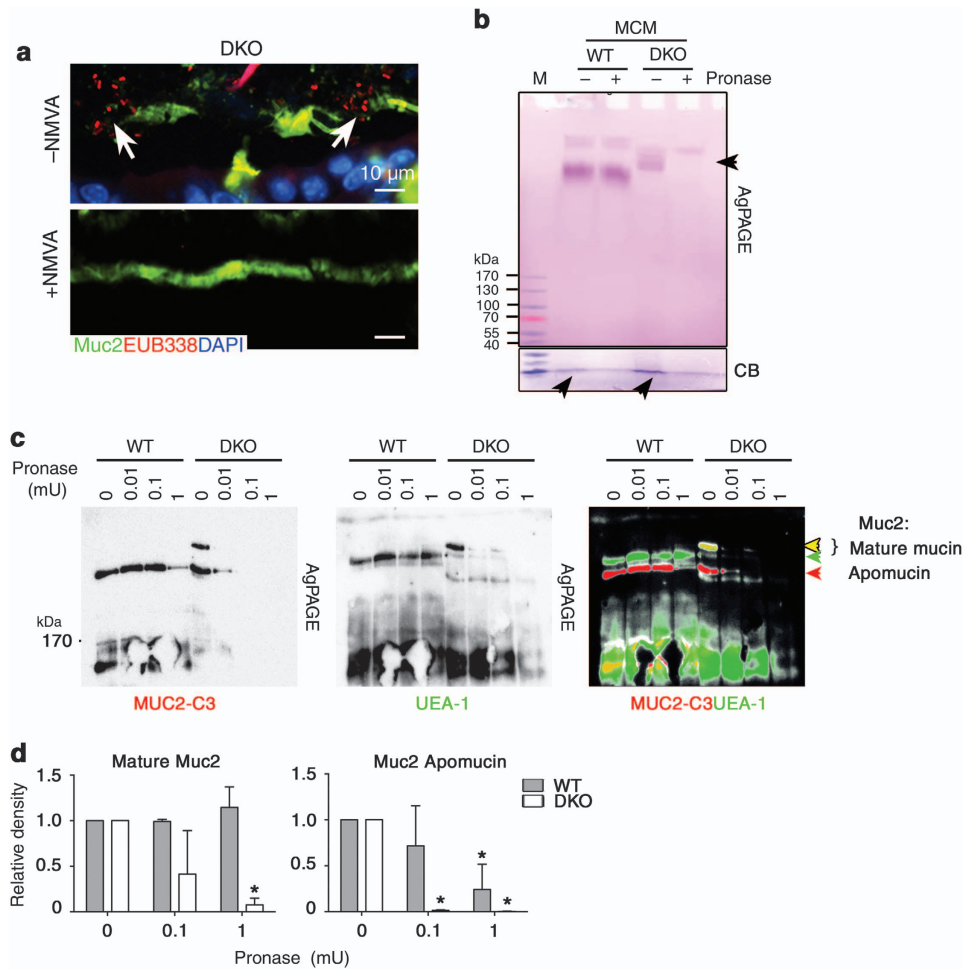


Figure 6 O-glycans protect Muc2 from bacterial protease-mediated degradation. **(a)** Dual Muc2/fluorescence *in situ* hybridization staining. Note: images are from mice on a gel-food diet, which allowed preservation of broken mucus in untreated DKO mice. Arrows, bacteria. **(b)** Periodic acid/Schiff-stained composite agarose-polyacrylamide gel electrophoresis gel of mucin derived from streptomycin-treated mice. CB, Coomassie Blue loading control. **(c)** Western blotting for Muc2 protein (α Muc2-C3) and Fucosylated Muc2 (*Ulex europaeus* agglutinin-1). **(d)** Densitometry of mature and immature Muc2 bands in wild-type and DKO mice. Error bars, s.e.m. Degradation studies are representative of three separate experiments, the third with independently derived mucin samples. * $P < 0.05$ vs. 0 mU, Student's *t*-test.

analysis by AgPAGE and PAS staining revealed a minimal effect of pronase on WT mucus, demonstrated by a modest downward shift of the high MW band. In contrast, pronase treatment led to a dramatic loss of the high MW PAS-stained band compared with non-treated DKO mucus (**Figure 6b**).

To confirm this effect on the Muc2 mucin, we repeated the assay on isolated WT and DKO mucin treated with increasing doses of pronase, followed by western blotting using the UEA1 lectin to analyze mature (glycosylated) Muc2 and an anti-Muc2-C3 antibody (against Muc2 C-terminus) that recognizes total (glycosylated and unglycosylated) Muc2.⁸ This approach was necessary because the Muc2-C3 antibody has greater affinity toward less glycosylated mucin (see **Supplementary Figure S5a,b,d**), whereas UEA1 readily binds mature mucin from WT and DKO mice (see **Supplementary Figure S5c,d**). Of note, mucosal extractions also included an ~500 kDa non-glycosylated Muc2 band (i.e., negative for PAS, UEA1, and Tn

antigen) (see **Supplementary Figure S5b–d**), likely the intracellular Muc2 apomucin from sloughed epithelial cells found in secretions or deglycosylated by bacteria.

Pronase treatment revealed that mature (UEA1⁺) WT Muc2 remained intact even at the highest dose of 1 mU, whereas the UEA1⁺ Muc2⁺ band from DKO mucin began to degrade at the lowest dose (0.01 mU) and completely vanished at the 1 mU dose, consistent with the PAS staining (**Figure 6c**). Importantly, the non-glycosylated Muc2 band was degraded in both WT and DKO samples (**Figure 6c**), providing an internal control for protease activity and proof of principle that core 1- and 3-derived O-glycans afford protection against proteolysis. In addition, this non-glycosylated Muc2 protein showed a faster rate of degradation in DKO vs. WT mucin preparations in response to increasing levels of pronase, suggesting that the glycosylation status of the mature mucin could provide protection for the unglycosylated mucin against proteolytic attack (**Figure 6c**). Densitometry indicated that DKO Muc2

was between 10–100-fold more susceptible to degradation by pronase than WT Muc2 (Figure 6d).

Taken together, these results reveal that loss of mucin-type O-glycans renders Muc2 more susceptible to bacterial-derived proteolytic degradation, which in turn protects the mucosa from bacteria-induced inflammation.

DISCUSSION

The mucus layer has a key barrier role in the colon where the resident microbiota exists at the highest density and diversity relative to other regions of the intestine.²⁷ O-glycans are the major components of the polymeric Muc2 mucin that forms this mucus layer. Our study reveals that the two major types of O-glycans, core 1- and 3-derived O-glycans, are differentially expressed in the colon and collectively contribute to mucus layer integrity and prevent microbiota-driven colitis. Mechanistically, core 1- and 3-derived O-glycans promote mucin stability in the presence of bacterial-derived proteases. This critical function preserves mucus barrier integrity and prevents the unrestricted access of the microbiota to the mucosa that would otherwise lead to spontaneous chronic inflammation.

We found that C3GnT expression was higher in the proximal compared to the distal colon, in contrast to C1GalT1 expression that was highly expressed throughout the colon. This new finding explains why the colitis phenotype is mainly limited to the distal colon of IEC *C1galt1*^{-/-} mice, whereas colitis occurs throughout the colon in DKO mice. Interestingly, colitis in proximal colonic regions of DKO mice was less severe than in the distal colon. It is possible that this phenotype may be linked to region-specific microbiota communities as differences in abundance and diversity of the mucosa-associated microbiota in the proximal vs. distal regions have been reported.^{28,29} Regardless, our results underscore the essential role of O-glycosylation in general in regulating homeostasis of the colonic mucus layer.

Our data show that the degree of O-glycosylation directly impacts the ability to maintain a functional mucus layer in the presence of the microbiota in the colon. How do O-glycans preserve mucus integrity? Glycosidase activity is an inherent aspect of the microbiota, which has key roles in maintenance of some community members who ferment it for energy and catabolize it to modulate their cell walls.^{30–32} We observed rescue of N-glycosylated mucus after antibiotic treatment, suggesting that bacteria-derived glycosidases may break down or inhibit further modifications of the residual GalNAc structures on mucins from the DKO colon. Muc2 of the DKO colon still has the GalNAc structure. However, our data show that this residual structure is not sufficient to protect Muc2 from degradation in the colon where microbiota-derived glycosidases and proteases readily break down the core 1- and 3-deficient Muc2. This is of relevance in human UC, where, in addition to O-glycan defects, increased overall mucolytic activity of fecal contents was observed compared with healthy controls,²⁵ therefore likely rendering UC mucus more unstable and susceptible to breach.

Although our findings support that O-glycans function primarily to promote Muc2 stability, it is possible that O-glycosylation also influences establishment of a stable mucus layer. For example, mucin-type O-glycosylation has been linked to promoting optimal secretion of proteins that protect the digestive tract of *Drosophila* larvae.³³ In our study, we observed a relatively intact mucus layer in neonatal DKO pups (P7) or in adult DKO mice with greatly diminished bacteria after antibiotic treatment, supporting that mucin secretion is not significantly impaired in the absence of both types of O-glycans. Nevertheless, as the mucus layer is constantly renewed and degraded, further studies are needed to determine any possible role of O-glycosylation in regulating the maturation and trafficking of Muc2 and/or other mucus-associated proteins to promote the homeostasis of the mucus layer.

Recent studies have shown that O-glycans influence microbiota composition; for example, induced loss of C1GalT1 alters microbial communities in the distal colon.^{34,35} Similar findings were reported with mice deficient in fucosyltransferase 2 (Fut2) responsible for terminal fucosylation of glycans and the galactosyltransferase β 4GalT2 that forms the terminal Sd(a)/Cad carbohydrate antigen.^{36,37} The basis for this selection and whether glycan-mediated influences on microbiota composition reflect a dysbiotic community that potentiates colitis is unclear, although Fut2 deficiency has recently been linked to Crohn's disease.^{37,38} However, it is notable among genetic studies with targeted deletion of glycosyltransferases that, to our knowledge, only lack of C1GalT1 has been shown to overtly impact mucus layer structure and elicit spontaneous colitis. This suggests a preeminent role of mucus barrier function vs. other functions in promoting homeostatic interactions with intestinal microbiota. However, it remains to be addressed whether unique bacterial species, perhaps influenced by O-glycosylation, are required for mucus breakdown and/or colitis development.

Although all mucins, including membrane bound and secreted forms, require core 1 and 3 O-glycosylation, the Muc2 mucin appears to be the most critical. Several mucin-deficient mouse lines have been reported (e.g., Muc1, Muc13), but only deletion of Muc2 results in spontaneous disease similar to DKO mice.^{12,39} The dynamics of disease progression differ between DKO and *Muc2*^{-/-} mice: colitis is evident between 1 and 2 weeks in DKO (on a C57BL/6J or mixed B6/129Sv background) mice, but only by 8 weeks in *Muc2*^{-/-} mice on a B6 background.³⁹ This difference may be due to the fact that loss of core 1 and 3 O-glycans in DKO causes defects in many mucins, including Muc2. Indeed, membrane-bound mucins such as Muc1 and Muc13 have been shown to be important for intestinal barrier function during pathogen infection.^{40,41} However, environmental influences (e.g., facility-dependent microbial communities) may also readily explain the differences in Muc2 and intestinal O-glycan-deficient mice, as disease dynamics in *Muc2*^{-/-} and DKO mice from the same facility have not yet been compared side by side. Regardless, our findings add crucial insights into how the colonic mucus layer is maintained when Muc2 expression is intact, namely, through

core 1- and 3-derived O-glycan-mediated Muc2 stabilization in the colon.

The innate immune system directly responds to microbial-derived signals through pattern-recognition receptors such as Toll-like receptors (TLRs) and Nod-like receptors, although their roles in microbiota-induced disease appears contingent upon the genetic defect predisposing to colitis. For example, spontaneous colitis in *Il10*^{-/-} mice⁴² or IEC *IKK γ* ^{-/-} mice is dependent on TLR signaling by the microbiota. Conversely, spontaneous colitis in *Il2*^{-/-} mice is completely independent of TLR signaling,⁴² and deficiency of some TLRs (TLR5) can itself predispose to spontaneous colitis.⁴⁴ Interestingly, our previous report shows that the initiation of spontaneous colitis in IEC *C1galt1*^{-/-} mice was independent of most TLR-dependent signaling, including TLR4.¹⁰ In a separate study, we recently found that spontaneous colitis in DKO mice was controlled by caspase 1-dependent inflammasomes (Bergstrom *et al.*, unpublished). As DKO mice exhibit UC-like colitis, delineating the innate pathways that drive disease will provide insights into how mucus layer regulates homeostasis with the resident microbiota.

Collectively, these findings provide insights into the regulation of colon homeostasis by mucin-type O-glycans and lend key insights into the basis and pathogenic potential of similar mucus defects observed in UC. By promoting the formation of a stable mucus network overlying the epithelium, core 1- and 3-derived O-glycans preserve a mutualistic interaction with resident microbiota that keeps immune responses below their threshold of activation. In addition, compared with other colitis mouse models, the DKO develop reproducible colitis on either C57BL/6J or mixed B6/129Sv. Therefore, it provides not only a more clinically relevant opportunity to dissect how components of the microbiota or the immune system contribute to each stage of colitis pathogenesis but also a valuable model to test pharmacological interventions.

METHODS

Mouse breeding. WT and IEC *C1galt1*^{-/-} were generated by mating *C1galt1*-floxed (*C1galt1*^{fl/fl}) mice with VillinCre transgenic mice as described.¹⁰ To produce dual intestinal core 1- and core 3 O-glycan-deficient (DKO) mice, *C1galt1*^{fl/fl}; *C3GnT*^{+/-} females were crossed with *C3GnT*^{+/-}; *C1galt1*^{fl/fl}; VillinCre⁺ males to generate *C3GnT*^{-/-}; IEC *C1galt1*^{-/-}, DKO, and WT littermates. To induce a postnatal deficiency of O-glycans, *C3GnT*^{+/-}; *C1galt1*^{fl/fl} mice were first crossed with previously generated *C1galt1*^{fl/fl}; VillinCre-ER^{T2} (TM-IEC *C1galt1*^{fl/fl}) mice¹⁰ on a *C3GnT*^{+/-} background to generate TM-IEC *C1galt1*^{fl/fl}; VillinCre-ER^{T2}, TM-IEC *C1galt1*^{fl/fl}; *C3GnT*^{-/-}; VillinCre-ER^{T2}, and WT (TM-IEC *C1galt1*^{fl/fl}) littermates. To generate TM-IEC *C1galt1*^{-/-} and TM IEC *C1galt1*^{-/-}; *C3GnT*^{-/-} (TM-DKO) mice, 10–12-week-old mice were injected intraperitoneally with 1 mg TM (MP Bio-medicals, Solon, OH) in an ethanol/sunflower seed oil mixture (1:9 (v/v)) for 5 consecutive days. All mice are on a C57BL/6J and 129/SvImJ mixed background, except for the TM-inducible lines, which are on a B6 congenic background. Animals were fed standard chow (PicoLab Rodent Diet 20; LabDiet, St. Louis, MO). All animal studies were carried out in a specific pathogen-free environment according to animal welfare regulations stipulated by Institutional Animal Care and Use Committee.

Tissue preservation and histology. For histology, tissues were freshly harvested from mice and fixed with 10% neutral buffered formalin or in Carnoy's fixative (60% methanol, 30% chloroform, and 10% acetic acid) prior to paraffin embedding. Paraffin-embedded sections (5 μ m) were stained with hematoxylin and eosin. The pictures were obtained with a Nikon Eclipse E600 microscope equipped with a Nikon DS-2Mv camera, using the software NIS -Elements AR (V3.0) (All from Nikon Instruments; Lewisville, TX). Histological severity of colitis was determined as described below.

Histological scoring. Histologic scoring was performed using a modified protocol from Haezelwood *et al.* (2008).⁴⁸ The following parameters and their respective scoring is as follows: polymorphonuclear cell infiltration per high-power field (HPF; 40 \times) (0–5 = 0; 6–10 = 1; 10–20 = 2; >20 = 3); mononuclear cell infiltration per HPF (None (<1 \times WT) = 0; Mild (1–2 \times WT) = 1; Moderate (2–3 \times WT) = 2; Severe (>3 \times WT) = 3); mucosal hyperplasia (<1 \times thickness of WT = 0; 1–1.5 \times thickness of WT = 1; 1.6–2 \times WT = 2; >2 \times WT = 3); goblet cell loss (<10% loss vs. WT = 0; 11–25% loss vs. WT = 1; 25–50% loss vs. WT = 2; >50% loss vs. WT = 3); and crypt abscesses (no. per section: 0 = 0, 1–5 = 1, 6–10 = 2, >10 = 3). The highest score to be obtained is 15. Scoring was performed under blinded conditions by an independent observer. For polymorphonuclear and mononuclear cell infiltration, and goblet cell enumeration, the mean value over 4–5 HPFs was determined and used for the final value. For mucosal thickness assessment, the mean value for each section was taken from 8 to 10 digital measurements over regular intervals of the length between the muscularis mucosa and the surface epithelium.

Histological staining of mucins. Carnoy's-fixed sections were cut (5 μ m), deparaffinized, and hydrated using standard protocols. Sections were then immersed with AB pH 2.5 (Newcomer Supply, Middleton, WI), which stains acidic mucins a light blue,¹⁰ for 20 min and then thoroughly rinsed in tapwater. Sections were counterstained with nuclear fast red for 10 min, dehydrated, mounted with Permount, and imaged.

Immunostaining. Formalin- or Carnoy's-fixed paraffin-embedded sections were deparaffinized and rehydrated. For Streptavidin-biotin-based staining, sections were first blocked with Streptavidin/Biotin Blocking Solution (Vector Laboratories, Burlingame, CA). For IHC, endogenous peroxidase blocking was performed by incubation with 3% H₂O₂ for 10 min at room temperature (RT). For IF or IHC, Serum-Free Protein Block (DAKO, Carpinteria, CA) was used to block non-specific antibody binding (10 min, RT). Following blocking, sections were incubated with rabbit anti-MUC2 (H300 Santa Cruz, Dallas, TX), and/or biotinylated mouse anti-Tn antigen IgM (provided by Tongzhong Ju and Richard Cummings, Emory University, Atlanta, GA), or rabbit anti myeloperoxidase (5 μ g ml⁻¹, ThermoFisherScientific, Waltham, MA), overnight at 4 °C. For anti-myeloperoxidase detection, sections were stained with Cy-3-labeled goat anti-rabbit IgG (1:50; Jackson ImmunoResearch Laboratories, West Grove, PA). For MUC2 IF staining, sections were incubated with biotinylated goat anti-rabbit IgG (1.5 μ g ml⁻¹) and then with DyLight 488-labeled Streptavidin (ThermoFisherScientific; 5 μ g ml⁻¹) for 30 min at RT. For dual Muc2-Tn epifluorescence, sections were incubated with Cy-3-labeled goat anti-rabbit IgG and DyLight 488-labeled Streptavidin. Sections were then counterstained with 25 ng ml⁻¹ 4,6-diamidino-2-phenylindole in dH₂O for 3 min, then washed with dH₂O, and mounted using PermaFluorAntifade (ThermoFisherScientific). For anti-Tn antigen IHC, sections were incubated with horseradish peroxidase (HRP)-conjugated Streptavidin (2 μ g ml⁻¹; Jackson ImmunoResearch Laboratories) for 40 min at RT, detected using the 3,3'-Diaminobenzidine Staining Kit (Vector Laboratories, Burlingame, CA), and counterstained with hematoxylin, dehydrated, and mounted. For epifluorescent imaging, specimens were analyzed with a Nikon Eclipse 80i microscope (USA) equipped

with a Nikon DS-Qi1MC camera operating through NIS Elements AR software (v3.0). For imaging IHC staining, sections were imaged by brightfield as above. Species-specific, isotype control antibodies or non-primary antibody-treated sections were used for negative controls.

FISH and dual Muc2/FISH labeling. For FISH, stool pellet-containing colon sections fixed with Carnoy's fixative were incubated with Texas red-conjugated universal bacterial probe EUB338 (5'-GCTGCCTCCGTAGGAGT-3'; bp 337–354 in bacteria EU622773) or with a nonspecific probe (NON338 5'-ACTCCTACGGGAGGCAGC-3') as a negative control, (both from Eurofins MWG Operon, Louisville, KY) in hybridization buffer (20 mM Tris-HCl, pH 7.4; 0.9 M NaCl; 0.1% sodium dodecyl sulfate (SDS)) at 37 °C overnight. The sections were rinsed in wash buffer (20 mM Tris-HCl, pH 7.4; 0.9 M NaCl) at 37 °C for 15 min. For dual Muc2-FISH labeling, sections were stained with Muc2 as above prior to FISH.

Calculation of mucus thickness. For determination of mucus thickness using AB- or Muc2-stained tissue sections, 15–30 measurements were taken from each animal colon preserved in Carnoy's fixative. Each measurement was taken perpendicular to the upper and lower borders of the inner mucus layer, which are clearly delineated when this layer is well preserved. ImageJ software⁴⁹ was used for data acquisition. For each time point, the mean absolute value from each mutant mouse was divided by that of each WT mouse and multiplied by 100 to get a percentage of thickness relative to WT mice, and then an average percentage of thickness was obtained for each mutant mouse. The final values are the mean percentage of thickness of mutant vs. WT mice, which are assigned a value of "100%".

Antibiotic treatment. Mice were given filter sterilized (0.22 µm) tap water containing 1 g l⁻¹ each of metronidazole, neomycin sulfate, ampicillin, and 0.5 g l⁻¹ of vancomycin (Sigma-Aldrich, St. Louis, MO),¹⁰ and 0.1% sucrose. Control mice were given water with 0.1% sucrose. After 3–4 weeks, mice were killed. For streptomycin treatment, mice were orally gavaged with 20 mg streptomycin in a 100 µl volume in sterile ddH₂O, once per day for 2 days, and then killed.

Bacterial enumeration. Total bacteria was enumerated by real-time qPCR for the gene encoding the highly conserved region of the 16S rRNA gene using the universal primers we have already optimized.¹⁰ DNA was extracted from 100 mg of stool using the Qiagen Stool Mini (Qiagen, Valencia, CA). SYBR-green-based qPCR was performed using primers described below.

Mucus isolation. Colons from WT and O-glycan-deficient mice were opened up longitudinally, and stool contents were carefully removed. Adherent mucus was gently scraped off with a glass slide, using gentle pressure. Secretions were placed in a microtube along with 0.2 ml ice-cold phosphate-buffered saline (PBS) containing 2 × complete protease inhibitors (Life Sciences, Roche; Branford, CT), and five volumes of guanidium chloride extraction buffer (6 M GuCl, 0.1 M Tris pH 8.0, 1 mM EDTA) was added. The secretions were dispersed with a Dounce (ThermoFisherScientific) homogenizer (ThermoFisherScientific) (three strokes) and then extracted overnight at 4 °C on a rotator. Following extraction, sample were reduced twice with 100 mM dithiothreitol, once for 5 h, and the other for overnight at 37 °C to solubilize the gel-forming mucin. The mucus was then alkylated with 250 mM iodoacetamide on a rotator overnight at RT, in the dark. The reduced and alkylated mucin was dialyzed into ddH₂O, and the postdialyzed sample was concentrated by centrifugation with an Amicon Centrifugal Filtration Unit, 100 kDa MWCO (EMD Millipore, Billerica, MA). The concentrated sample was then stored at –20 °C until analyzed.¹⁹

Composite SDS AgPAGE. Composite agarose-polyacrylamide gel is used to analyze large MW glycoproteins.⁴⁵ This is made up of a gradient of 0.5–1.0% agarose, 0–10% glycerol, and 0–6% acrylamide.⁴⁵

Mucins were electrophoresed for 4 h at 30 mA on ice, and the gels were processed for further analysis via PAS staining, using the Pierce Glycoprotein Staining Kit (ThermoFisherScientific). Gels were imaged on an Epson scanner (Long Beach, CA).

Mucus degradation assay. Semi-purified mucin was quantified by Dc Protein Assay (Bio-Rad, Hercules, CA, USA). Five micrograms of WT and DKO mucin were treated with PBS or 0.01–1 mU pronase (Calbiochem; EMD Millipore, Billerica, MA) and incubated for 30 min in 1 × PBS pH 7.0 at 37 °C in a 30-µl volume. Sample buffer (6 ×) was then added, and samples were boiled for 5 min to deactivate the pronase, then separated by AgPAGE, and analyzed by in-gel staining with periodic acid/Schiff and western blotting.

Western blotting, densitometry, and membrane overlays. Mucin samples separated by AgPAGE were transferred onto a polyvinylidene difluoride membrane via wet transfer at 100 V for 1.5 h on ice. The membrane was blocked with 5% milk in TBS-T (pH 7.6) and then incubated with polyclonal rabbit anti-Muc2-C3 antisera⁸ (1:1000) overnight at 4 °C. Membranes were washed with TBS-T, incubated with HRP-conjugated goat anti-rabbit IgG for 1 h at RT, washed, detected with SuperSignal Enhanced Chemiluminescence reagent (ThermoFisherScientific), and developed using film and/or a G:Box gel doc system (Syngene, Frederick, MD). For subsequent blotting for fucosylated glycans, membranes were stripped using 0.1% SDS, 0.2 M Glycine, 1% Tween 20, pH 2.2, and reblocked as above, as well as with the Streptavidin/Biotin Blocking Kit (Vector Laboratories, Burlingame, CA, USA) and probed with biotin-conjugated UEA1 (2 µg ml⁻¹) for 2 h at RT, washed, then incubated with HRP-conjugated Streptavidin (Jackson ImmunoResearch Laboratories, West Grove, PA; 2 µg ml⁻¹) for 40 min, detected, and visualized as above. Densitometry was performed on inverted grayscale images using the ImageJ software and analyzed using the Excel (Microsoft, Redmond, WA) and Prism (GraphPad, San Diego, CA) software. For membrane overlays, blot images of Muc2 and UEA1 (analyzed on the same blot) were opened in Adobe Photoshop CS3 (San Jose, CA), inverted, false colored using the Adjustments → Selective color option in the Image pull down menu, and overlaid by adjusting the opacity of the top layer. Markers were used for precise alignments.

RNA and gDNA extraction and RT-qPCR. Total RNA was extracted from flash-frozen colon tissue using the RNeasy Kit (Qiagen) and 1.5 µg was reverse transcribed using the Omniscript RT Kit (Qiagen) according to the manufacturer's instructions. For bacterial 16S rRNA analysis, bacterial gDNA was extracted from mouse fecal pellets using the Stool Mini Kit (Qiagen) and 5 ng was used for PCR. qPCR was performed using 2 × iQ MasterMix and a CFX-96 system (Bio-Rad). Cytokine primer sequences are *tnf* Fwd: 5'-CATCTTCTCAAATTC GAGTGACAA-3', Rev: 5'-TGGGAGTAGACAAGGTACAACCC-3'; *il6* Fwd: 5'-GAGGATACCACTCCCAACAGACC-3', Rev: 5'-AAGT GCATCATCGTTGTTTCAT-3'; *il1beta* Fwd: 5'-CAGGATGAGGACA TGAGCACC-3', Rev: CTCTGCAGACTCAAACCTCCAC-3'; and 18S rRNA Fwd: 5'-GTAACCCGTTGAACCCATT-3', Rev: 5'-CCATCC AATCGGTAGTAGCG-3'. Group-specific primers for Bacteroidales order, *Lactobacillus* sp., *Bifidobacterium* sp., and *Clostridium* sp. were obtained from Wlodarska *et al.*⁴⁶ and *Prevotella* sp. were obtained from Matsuki *et al.*⁴⁷ Expression analysis was carried out using the Bio-Rad CFX manager 3.0 (using the $\Delta\Delta$ Ct method for relative normalized expression and Δ Ct for relative expression). All relative normalized expression data used 18S rRNA mRNA as the internal control.

Statistics. Data was plotted and analyzed using GraphPad Prism V5.0 (San Jose, CA). Error bars represent s.d. unless otherwise indicated. All data sets passed the D'Agostino and Pearson omnibus K2 normality tests. Student's *t*-test was used to analyze the difference between two groups. One-way analysis of variance followed by Bonferroni post-test was used to analyze the difference between ≥ 3 groups. A *P*-value < 0.05 was considered to be significant.

SUPPLEMENTARY MATERIAL is linked to the online version of the paper at <http://www.nature.com/mi>

ACKNOWLEDGMENTS

We thank Dr Courtney Griffin for technical support. This work was supported by NIH grants RR018758, R01DK085691, UL1TR000124, and U01AI095473; Chinese National Natural Science Foundation grants 81470825, 8151001178, 31400692, and 81172299; Swedish Research Council, The Swedish Cancer Foundation, The Knut and Alice Wallenberg Foundation; and the Crohn's and Colitis Foundation of America Research Fellows Award 285148.

AUTHOR CONTRIBUTIONS

K.B., J.F., M.E.V.J., G.C.H., and L.X. designed the experiments; K.B., and M.E.V.J. and Q.W. conducted the experiments; K.B., M.E.V.J., J.F., G.C.H., and L.X. analyzed the data; X.L., N.G., J.S., J.M.M., and S.M. provided technical help; W.C., and J.B. critiqued the manuscript. K.B., J.F., and L.X. wrote the manuscript.

DISCLOSURE

The authors declared no conflict of interest.

© 2016 Society for Mucosal Immunology

REFERENCES

- Ford, A.C., Moayyedi, P. & Hanauer, S.B. Ulcerative colitis. *BMJ* **346**, f432 (2013).
- Strober, W., Fuss, I. & Mannon, P. The fundamental basis of inflammatory bowel disease. *J. Clin. Invest.* **117**, 514–521 (2007).
- Johansson, M.E., Sjovall, H. & Hansson, G.C. The gastrointestinal mucus system in health and disease. *Nat. Rev. Gastroenterol. Hepatol.* **10**, 552–361 (2013).
- Ley, R.E., Peterson, D.A. & Gordon, J.I. Ecological and evolutionary forces shaping microbial diversity in the human intestine. *Cell* **124**, 837–848 (2006).
- Pelaseyed, T. *et al.* The mucus and mucins of the goblet cells and enterocytes provide the first defense line of the gastrointestinal tract and interact with the immune system. *Immunol. Rev.* **260**, 8–20 (2014).
- Ambort, D. *et al.* Calcium and pH-dependent packing and release of the gel-forming MUC2 mucin. *Proc. Natl. Acad. Sci. USA* **109**, 5645–5650 (2012).
- Johansson, M.E., Holmen Larsson, J.M. & Hansson, G.C. The two mucus layers of colon are organized by the MUC2 mucin, whereas the outer layer is a legislator of host-microbial interactions. *Proc. Natl. Acad. Sci. USA* **108** (Suppl 1), 4659–4665 (2010).
- Johansson, M.E. *et al.* The inner of the two Muc2 mucin-dependent mucus layers in colon is devoid of bacteria. *Proc. Natl. Acad. Sci. USA* **105**, 15064–15069 (2008).
- Allen, A., Hutton, D.A. & Pearson, J.P. The MUC2 gene product: a human intestinal mucin. *Int. J. Biochem. Cell. Biol.* **30**, 797–801 (1998).
- Fu, J. *et al.* Loss of intestinal core 1-derived O-glycans causes spontaneous colitis in mice. *J. Clin. Invest.* **121**, 1657–1666 (2011).
- Larsson, J.M.H. *et al.* Altered O-glycosylation profile of MUC2 mucin occurs in active ulcerative colitis and is associated with increased inflammation. *Inflamm. Bowel Dis.* **17**, 2299–2307 (2011).
- Van der Sluis, M. *et al.* Muc2-deficient mice spontaneously develop colitis, indicating that MUC2 is critical for colonic protection. *Gastroenterology* **131**, 117–129 (2006).
- An, G. *et al.* Increased susceptibility to colitis and colorectal tumors in mice lacking core 3-derived O-glycans. *J. Exp. Med.* **204**, 1417–1429 (2007).
- Brockhausen, I. *Biosynthesis of Mucin-Type O-glycans in Comprehensive Glycoscience* Editor-in-Chief: J.P. Kamerling; eds G Boons *et al.* Vol. 3: 33–59 (Elsevier, Boston, USA, 2007).
- Xia, L. *et al.* Defective angiogenesis and fatal embryonic hemorrhage in mice lacking core 1-derived O-glycans. *J. Cell. Biol.* **164**, 451–459 (2004).
- Hang, H.C. & Bertozzi, C.R. The chemistry and biology of mucin-type O-linked glycosylation. *Bioorg. Med. Chem.* **13**, 5021–5034 (2005).
- Robbe, C., Capon, C., Coddeville, B. & Michalski, J.-C. Structural diversity and specific distribution of O-glycans in normal human mucins along the intestinal tract. *Biochem. J.* **384**, 307–316 (2004).
- Rakoff-Nahoum, S., Paglino, J., Eslami-Varzaneh, F., Edberg, S. & Medzhitov, R. Recognition of commensal microflora by toll-like receptors is required for intestinal homeostasis. *Cell* **118**, 229–241 (2004).
- Png, C.W. Mucolytic bacteria with increased prevalence in IBD mucosa augment in vitro utilization of mucin by other bacteria. *Am. J. Gastroenterol.* **105**, 2420–2428 (2010).
- Norrsell, H., Bengtsson, J., Jovall, P.A. & Hansson, G.C. N-linked glycopeptides with blood group determinants lacking neuraminic acid from the epithelial cells of rat small and large intestine. *Eur. J. Biochem.* **203**, 285–293 (1992).
- Barthel, M. *et al.* Pretreatment of mice with streptomycin provides a *Salmonella* enterica serovar Typhimurium colitis model that allows analysis of both pathogen and host. *Infect. Immun.* **71**, 2839–2858 (2003).
- Bergstrom, K.S. *et al.* Muc2 protects against lethal infectious colitis by disassociating pathogenic and commensal bacteria from the colonic mucosa. *PLoS Pathog.* **6**, e1000902 (2010).
- Waksman, S.A. Streptomycin: background, isolation, properties, and utilization. *Science* **118**, 259–266 (1953).
- Miller, C.P. & Bohnhoff, M. Changes in the mouse's enteric microflora associated with enhanced susceptibility to *Salmonella* infection following streptomycin treatment. *J. Infect. Dis.* **113**, 59–66 (1963).
- Rhodes, J.M., Gallimore, R., Elias, E., Allan, R.N. & Kennedy, J.F. Faecal mucus degrading glycosidases in ulcerative colitis and Crohn's disease. *Gut* **26**, 761–765 (1985).
- Dwarakanath, A.D. *et al.* Faecal mucinase activity assessed in inflammatory bowel disease using ¹⁴C threonine labelled mucin substrate. *Gut* **37**, 58–62 (1995).
- Xu, J. & Gordon, J.I. Inaugural article: honor thy symbionts. *Proc. Natl. Acad. Sci. USA* **100**, 10452–10459 (2003).
- Wang, Y. *et al.* Regional mucosa-associated microbiota determine physiological expression of TLR2 and TLR4 in murine colon. *PLoS One* **5**, e13607 (2010).
- Hu, S. *et al.* Regional differences in colonic mucosa-associated microbiota determine the physiological expression of host heat shock proteins. *Am. J. Physiol. Gastrointest. Liver Physiol.* **299**, G1266–G1275 (2010).
- Sonnenburg, J.L. Glycan foraging in vivo by an intestine-adapted bacterial symbiont. *Science* **307**, 1955–1959 (2005).
- Martens, E.C., Roth, R., Heuser, J.E. & Gordon, J.I. Coordinate regulation of glycan degradation and polysaccharide capsule biosynthesis by a prominent human gut symbiont. *J. Biol. Chem.* **284**, 18445–18457 (2009).
- Martens, E.C., Chiang, H.C. & Gordon, J.I. Mucosal glycan foraging enhances fitness and transmission of a saccharolytic human gut bacterial symbiont. *Cell Host Microbe* **4**, 447–457 (2008).
- Zhang, L. *et al.* O-glycosylation regulates polarized secretion by modulating Tango1 stability. *Proc. Natl. Acad. Sci. USA* **111**, 7296–7301 (2014).
- Perez-Munoz, M.E. *et al.* Discordance between changes in the gut microbiota and pathogenicity in a mouse model of spontaneous colitis. *Gut Microbes* **5**, 286–295 (2014).
- Sommer, F. *et al.* Altered mucus glycosylation in core 1 o-glycan-deficient mice affects microbiota composition and intestinal architecture. *PLoS One* **9**, e85254–e85254 (2014).
- Kashyap, P.C. *et al.* Genetically dictated change in host mucus carbohydrate landscape exerts a diet-dependent effect on the gut microbiota. *Proc. Natl. Acad. Sci. USA* **110**, 17059–17064 (2013).
- Rausch, P. *et al.* Colonic mucosa-associated microbiota is influenced by an interaction of Crohn disease and FUT2 (Secretor) genotype. *Proc. Natl. Acad. Sci. USA* **108**, 19030–19035 (2011).
- McGovern, D.P.B. *et al.* Fucosyltransferase 2 (FUT2) non-secretor status is associated with Crohn's disease. *Hum. Mol. Genet.* **19**, 3468–3476 (2010).
- Wenzel, U.A. *et al.* Spontaneous colitis in Muc2-deficient mice reflects clinical and cellular features of active ulcerative colitis. *PLoS One* **9**, e100217 (2014).

40. Every, A.L., Chionh, Y.T., Skene, C.D., McGuckin, M.A. & Sutton, P. Muc1 limits *Helicobacter felis* binding to gastric epithelial cells but does not limit colonization and gastric pathology following infection. *Helicobacter* **13**, 489–493 (2008).
41. McAuley, J.L. *et al.* MUC1 cell surface mucin is a critical element of the mucosal barrier to infection. *J. Clin. Invest.* **117**, 2313–2324 (2007).
42. Rakoff-Nahoum, S., Hao, L. & Medzhitov, R. Role of Toll-like receptors in spontaneous commensal-dependent colitis. *Immunity* **25**, 319–329 (2006).
43. Nenci, A. *et al.* Epithelial NEMO links innate immunity to chronic intestinal inflammation. *Nature* **446**, 557–561 (2007).
44. Vijay-Kumar, M. *et al.* Deletion of TLR5 results in spontaneous colitis in mice. *J. Clin. Invest.* **117**, 3909–3921 (2007).
45. Johansson, M.E. & Hansson, G.C. Analysis of assembly of secreted mucins. *Methods Mol. Biol.* **842**, 109–121 (2012).
46. Wlodarska, M. *et al.* Antibiotic treatment alters the colonic mucus layer and predisposes the host to exacerbated *Citrobacter rodentium*-induced colitis. *Infect. Immun.* **79**, 1536–1545 (2011).
47. Matsuki, T. *et al.* Development of 16S rRNA-gene-targeted group-specific primers for the detection and identification of predominant bacteria in human feces. *Appl. Environ. Microbiol.* **68**, 5445–5451 (2002).
48. Heazlewood, C.K. *et al.* Aberrant mucin assembly in mice causes endoplasmic reticulum stress and spontaneous inflammation resembling ulcerative colitis. *PLoS medicine* **5**, e54 (2008).
49. Schneider, C.A., Rasband, W.S. & Eliceiri, K. W. NIH Image to ImageJ: 25 years of image analysis. *Nat Methods* **9**, 671–675 (2012).